

OBSERVATION OF SPONTANEOUS EMITTED X-RAY BETATRON RADIATION IN BEAM-PLASMA INTERACTIONS

Shuoqin Wang, C. E. Clayton, B. E. Blue, E. S. Dodd, C-K, Huang, K. A. Marsh, W. B. Mori, C. Joshi,
UCLA, CA 90095
S. Lee, P. Muggli, T. Katsouleas, USC, CA 90089
F. J. Decker, M. J. Hogan, R. H. Iverson, P. Riamondi, D. Walz and R. Siemann, SLAC, CA 94309
R. Assmann, CERN, Switzerland

Abstract

An experiment is being carried out at the Stanford Linear Accelerator Center (SLAC) to see if an ion channel can wiggle a beam of ultra-relativistic electrons to produce x-ray radiation. The goal is to create an intense source of undulator radiation using a plasma wiggler in the 1-10 KeV range and also to determine the suitability of such an electrostatic wiggler to create a coherent beam of x-rays via the ion channel laser mechanism[1]. Here we give some of the scaling laws for the power and frequency distribution of the spontaneous emission from sending an electron beam through such an ion channel. Some initial experimental observations are also presented.

1 INTRODUCTION

It is well known that a beam of relativistic (γ_b) electrons will undergo oscillations of its transverse envelope in an ion channel which exerts a transverse focusing force $F = 2\pi n_p e^2 r$ on the beam, where r is the initial displacement of the electron from the axis. The oscillation frequency of a single electron in this channel is the betatron frequency $\omega_\beta = \omega_p / \sqrt{2\gamma_b}$ where ω_p is the plasma frequency. As a result of this oscillation, the electrons radiate spontaneously with a broad spectrum that has a peak at $\omega_r = 2\gamma_b^2 \omega_\beta / (1 + K^2)$ with a cut-off frequency $\omega_c = 3\gamma_b^3 \omega_\beta^2 r / c$, where $K = \frac{1}{2} \gamma_b \omega_\beta r / c$ is the wiggler strength. As the number of undulating periods increases the radiated spectrum narrows as $\sim 1/N$ around ω_r . On the other hand, if $K > 1$, electrons distributed in a range of r radiate with different peak frequencies and therefore broaden the spectrum.

Assuming for the moment that an electron is r away with respect to the axis, the transverse $\beta_r \equiv \dot{r} / c = r k_\beta \cos(\omega_\beta t)$ and the transverse acceleration $\dot{\beta}_r$ therefore is proportional to ω_β^2 . Since the total

synchrotron power emitted is proportional to $\dot{\beta}_r^2$, this is proportional to ω_β^4 or square of the plasma density n_p . The divergence angle of the emitted radiation is about $2K/\gamma_b$ which for the ultra-relativistic beam can be very narrow.

2 EXPERIMENT

The experiment to measure betatron x-ray emission from an ion channel was carried out at SLAC parasitically to the Plasma Wakefield Acceleration experiment, E157 [2]. The general experimental set-up has been described in [2]. Basically the 28.5 GeV electron beam containing 2×10^{10} particles is focused to a spot diameter of $\sigma_r = 30 \mu\text{m}$ at the entrance of a 1.4 m long plasma cell. The density of the plasma is varied from about 10^{12} cm^{-3} to $2 \times 10^{14} \text{ cm}^{-3}$. Over this range of plasma densities the peak beam density is greater than the plasma density. The beam thus blows out the plasma electrons (see Fig. 1) about 0.6 mm before the peak of the beam leaving behind a plasma ion column.

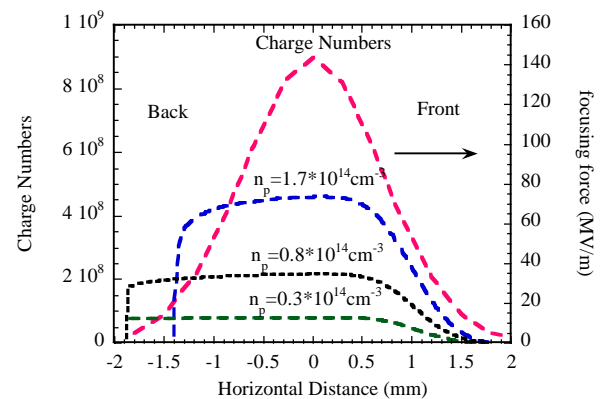


Figure 1: Beam charge distribution and the transverse force witnessed by the beam electrons σ_r away from the axis of ion channel from Particle-in-Cell simulation (Quasi-Static Appr.) at 3 different plasma densities.

The bulk of the electrons subsequently executes 1.5 envelope oscillations at a density of about $1.7 \times 10^{14} \text{ cm}^{-3}$. The head of the beam undergoes zero, one and two betatron oscillations as the channel is being dynamically formed (see Fig. 2).

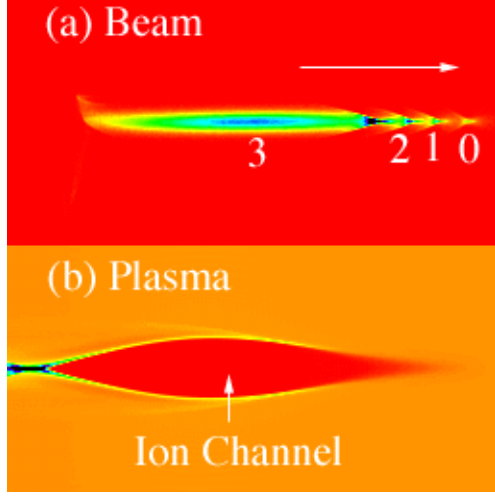


Figure 2: Evolution of (a) the beam and (b) the ion channel based on Particle-in-Cell simulation (Quasi-Static Approx.) with SLAC beam and plasma parameters [2]. 0,1,2 and 3 in (a) refer to the number of envelope oscillations made by different sections of the beam at the plasma exit.

As the beam envelope oscillates in this ion channel the electrons emit synchrotron radiation. We call this plasma betatron radiation which is emitted in a small forward cone angle. The radiation traverses 40 m of vacuum photon beam line, passing through two 75 μm beryllium and one 25 μm Ti (placed at 45°) foils before it impinges upon a silicon (111) crystal. The radiation scattered by the crystal is detected using two 1 mm thick silicon surface barrier detectors (SBD). One SBD is placed precisely at the Bragg angle to reflect 6.4 KeV x-ray, while the other was at a mismatched angle to receive Thomson-scattering x-rays from the electron clouds in the crystal lattice.

3 THEORY

The total radiated power due to synchrotron radiation [3] is

$$P(t) = \frac{2}{3} \frac{e^2}{c} \gamma^4 |\dot{\beta}|^2 \quad (1)$$

For a relativistic electron in an ion channel, the Newton equation of motion gives

$$r = r_0 \cos \phi \quad (2)$$

$$\beta_r = -r_0 k_\beta \sin \phi \quad (3)$$

$$\dot{\beta} \approx \dot{\beta}_r = -r_0 k_\beta \omega_\beta \cos \phi \quad (4)$$

based on the assumption that r_0 is the initial displacement and $d\phi/dt = \omega_\beta = \omega_p / \sqrt{2\gamma_0}$.

The total radiation energy is

$$E = \int P dt \propto k_\beta^4 \int_0^T \cos^2(\omega_\beta t) dt \propto k_\beta^4 \quad (5)$$

if T satisfies $\omega_\beta T = m\pi$, with T is the total time for a beam electron propagating through plasma in the lab frame. This is the condition at which we define transparency points. Since k_β is proportional to $\sqrt{n_p}$, the total radiated energy scales as plasma density squared. In an actual experiment photons with a certain frequency range are detected. In this case, the total detected energy must be found by integrating the frequency spectrum over the appropriate frequency range. The spectrum of radiated energy per unit frequency, per unit solid angle is

$$\frac{d^2 E_r(\omega, \Omega)}{d\omega d\Omega} = \frac{e^2 \omega^2}{4\pi^2 c} \left| \int \hat{n} \times (\hat{n} \times \bar{\beta}) e^{i\omega(t - \frac{\hat{n} \cdot \vec{r}}{c})} dt \right|^2 \quad (6)$$

Now we discuss what Thomson-scattering signal would be seen by the SBD in the experiment. The detectable photon energy at the lower end is mainly limited by the K-edge of the metallic foils that are placed in the path of the beam whereas the detectable photon frequency on the higher end is mainly limited by the photon passing through the detector itself. In other words, the Thomson-scattering signal received by the SBD can be expressed as

$$E_{SBD} = \int_0^\infty \frac{dE_{T-S}(\omega)}{d\omega} d\omega \quad (7)$$

with

$$E_{T-S}(\omega) \propto E_r(\omega) \cdot T_{air}(\omega) \cdot T_{Be}(\omega) \cdot T_{Ti}(\omega) \cdot f_{Si}(\omega) \quad (8)$$

where $T_{air}(\omega)$, $T_{Be}(\omega)$, $T_{Ti}(\omega)$ are the transfer functions of 0.5m air at room temperature, two 75 μm Be foils and one 37 μm Ti foil respectively, $f_{Si}(\omega)$ is the atomic scattering factor of a silicon atom, and $dE_r(\omega)/d\omega = \int dE_r(\omega, \Omega)/(d\omega d\Omega) d\Omega$, as shown in

Fig.3.

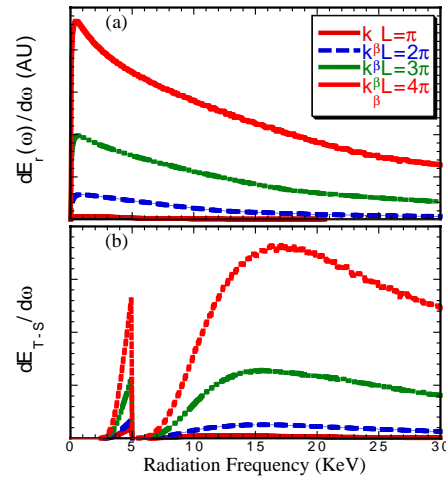


Figure 3: (a) Numerical integration of x-ray angular distribution to give $dE_r(\omega)/d\omega$ vs. ω . (b) Frequency spectrum including transfer functions.

Figure 4 shows the total expected x-ray energy yield at the four transparency points after integrating the four curves shown in Fig.3(b) over all frequencies.

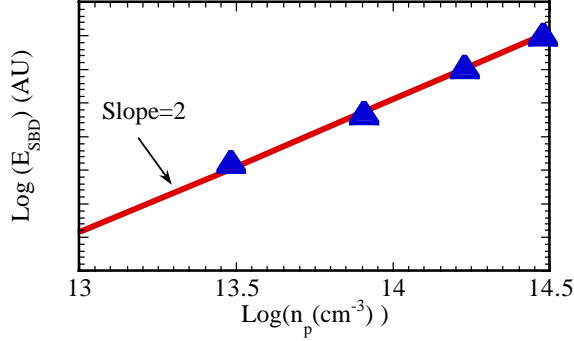


Figure 4: The total calculated radiation energy (triangles) incident on a SBD detector showing a quadratic dependence (solid line) on plasma density.

4 SAMPLE RESULTS

As mentioned earlier since the radiation spectrum at the spontaneous emission is rather broad, one needs some way to effectively reflect these x-rays so that they can be detected. We use both Bragg-scattering off an x-ray crystal, which is frequency specific at a given angle, and Thomson-scattering, which reflects a broad range of wavelengths at all angles. Figure 5 shows the relative efficiency of the two processes as measured by the total energy detected on a SBD detector by rotating the crystal angle. As for Thomson-scattering, the energy is proportional to the interaction length between photons and the silicon crystal, which is longer as the rotation angle is smaller. The sharp peak corresponds to the Bragg-scattering signal at 6.4 ± 0.13 KeV, with the uncertainty due to the resolution of the rotation stage and the width of the SBD.

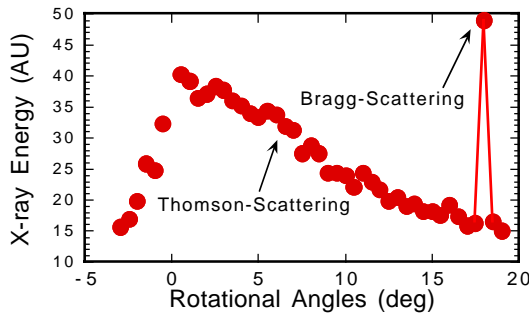


Figure 5: X-ray energy measured by the SBD as the function of rotation angle of the Si crystal with respect to the photon beam when the plasma is off.

In the experiment, the rotation angle was fixed at 18° with one SBD, D1, satisfying the Bragg-scattering condition while a second one, D2, at a different angle for collecting the broadband (Fig. 3(b)) Thomson-Scattering signal, which is broad-band as shown in Fig.3(b). As a matter of fact, the signal witnessed by D1 not only includes Bragg-scattering signal, but also includes Thomson-scattering signal from photons with incident angles not satisfying the Bragg-scattering condition. The latter part can be subtracted, in principle, by comparing to the Thomson signal received by D2. Figure 6 clearly shows Bragg-scattering signal received by D1 at the first transparency point ($k_\beta L \approx \pi$) while the Thomson-scattering signal received by D2 is still close to the noise level. The Bragg-scattering signal can be converted to the absolute value of photons with the assumption that all photons have the same photon energy, 6.4 KeV.

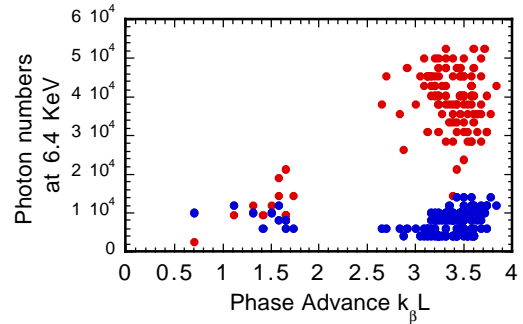


Figure 6: Signals on two SBD's at the first transparency point. Photon numbers are derived based on the Bragg-scattering condition. Open circles for D1, solid circles for D2.

As the plasma density increases, The Thomson-scattering signal should increase as expected in Fig.4. Detailed results will be published elsewhere.

The authors wish to thank W. H. Tompkins of SSRL and E. Esarey of LBNL for their help. This work was supported by DOE grants DE-AC03-76SF00515, DE-AC-03-76SF0098, and DE-FG03-98-DP-0021 and NSF grant ECS9617089.

5 REFERENCES

- [1] D. H. Whittum et al., Phys. Rev. Lett. 64, 2511, (1990).
- [2] M. Hogan et al., Phys. Plasmas, 7, 2241, (2000).
- [3] J. D. Jackson, "Classical Electrodynamics ", 2nd Edition, John Wiley & Sons, Inc., (1975).